Chapter 7

Synthetic Reactive Polyelectrolytes for Cell Encapsulation

M. A. Jafar Mazumder,[1,*] Nicholas A. D. Burke,[1] Feng Shen,[2] Terry Chu,[1] Murray A. Potter,[2] and Harald D. H. Stöver[1,*]

[1]Department of Chemistry, McMaster University, 1280 Main Street West, Hamilton, ON, Canada, L8S 4M1
[2]Department of Pathology & Molecular Medicine, McMaster University, 1200 Main Street West, Hamilton, ON, Canada, L8N 3Z5
[*]mazumdma@mcmaster.ca; stoverh@mcmaster.ca

In this work we studied the synthesis and characterization of reactive polyelectrolytes that are capable of forming covalent cross-links, and that can be used in cell encapsulation. In the first part we outline the synthesis and characterization of these polyelectrolytes, and their use to form covalently cross-linked outer shells around calcium alginate microcapsules. The second part presents the formation of covalently cross-linked networks within the cores of calcium alginate microcapsules. The encapsulation processes, capsule morphology, mechanical strength, permeability and biocompatibility are discussed in some detail. The resulting capsules showed improved mechanical strength yet remain cyto-compatible. This approach to cell-encapsulation may be useful for cell immuno-isolation in therapeutic cell transplants.

Introduction

Encapsulation of cells within semi-permeable polymer shells or beads is a potentially powerful tool for the treatment of enzyme deficiency disorders such as lysosomal storage disorders, neurological disorders, dwarfism, hemophilia, cancer and diabetes. Encapsulation of non-autologous cells can provide mechanical protection and immuno-isolation, permitting the use of standard cell lines that are genetically modified to express key enzymes or other actives missing in patients.

In Polymeric Delivery of Therapeutics; Morgan, S., et al.;
ACS Symposium Series; American Chemical Society: Washington, DC, 2010.

The capsule wall serves as a semi-permeable membrane that allows the exchange of oxygen, metabolites and release of therapeutic proteins, while obscuring the encapsulated cells from the host's immune system (*1–5*). These capsules need to be compatible with both host and implanted cells and should not degrade *in vivo*. This requires capsule walls with suitable molecular weight (MW) cut-off, and ideally some form of cross-linking to enhance resistance to biochemical and mechanical degradation.

The most common cell encapsulation approach involves the alginate/ poly-L-lysine/alginate (APA) capsules as first described by Lim and Sun (*5*). These capsules are primarily composed of alginate, an anionic polysaccharide isolated from marine brown algae. Alginates are linear binary copolymers of β-D-mannuronic acid (M) and α-L-guluronic acid (G) residues. Calcium ions are used to cross-link G-rich regions of the alginate chains, which leads to the formation of firm calcium alginate (CaAlg) hydrogel beads. The resulting CaAlg beads are coated with poly-L-lysine (PLL) to strengthen the outer bead surface and control permeability (*6*). A final coating with Na alginate (Alg) is applied in order to hide the cationic PLL from the host (*4*) and thus make the capsules biocompatible.

While APA capsules meet many of the requirements for immuno-isolation of cells when implanted into mice (*7*), they have at times shown insufficient strength when implanted into larger animals such as dogs, where they collapse within 2 weeks (*8*). This may be due to the destabilization of the alginate core matrix through slow exchange of calcium ions with other physiological ions and/or the loss or degradation of the polyelectrolyte overcoats (*9*, *10*).

A number of studies have attempted to address the challenge of long-term mechanical stability by varying the MW (*11*) or G/M ratio of the alginate (*4*, *12–14*), using uncoated alginate beads (*15*), different cross-linking ions (*14*, *16*) and polyelectrolytes (*17–20*) to coat alginate based capsules. Examples include Alg-chitosan-Alg (*21*), Alg-PLL-poly(acrylic acid) (*19*), Alg-PLL-poly(ethylene glycol), Alg-chitosan-poly(ethylene glycol), and Alg-PLL-poly(ethylene glycol)-Alg (*20*), Alg-poly-L-ornithine-Alg (*17*, *22*), Alg-poly(allylamine)-Alg (*23*), Alg-PEI- poly(acrylic acid)-PEI-Alg, and Alg-PEI-carboxymethylcellulose-PEI-Alg capsules (*24*).

A number of fully synthetic polymers such as poly(hydroxyethyl methacrylate-*co*-methyl methacrylate), p(HEMA-*co*-MMA) (*25*), poly(hydroxyl ethylmethacrylate-*co*-ethyl methacrylate), p(HEMA-*co*-EMA) (*26*) and polyphosphazene (PPP) (*2*) have been studied as biomaterials for microencapsulation.

Several groups have explored ways to improve the capsule strength by photo polymerization of (meth)acrylate-functionalized alginate (*13*, *27–30*) or of other monomers within the alginate core (*31*, *32*). Cross-linking of Alg-chitosan capsules with glutaraldehyde or carbodiimide was shown to improve their mechanical strength (*33*), though these small-molecule cross linkers raise serious toxicity issues. Photo polymerization of monomer-functionalized alginate (*13*, *27–30*), or of monomers within the alginate core (*31*, *32*), was used to strengthen the capsules, though irradiation and the presence of photo initiator and monomers again posed challenges to the encapsulated cells. Recently, Hallé and coworkers

(*34*, *35*) studied APA capsules in which a photoactivatable crosslinker was used to covalently link the PLL chains with other PLL chains and with adjacent alginate chains, in both the surface of the core and the outer coating. These capsules displayed greatly improved mechanical stability while maintaining the cell viability and permeability of standard APA capsules. In addition, these covalently cross-linked capsules prevented the escape of malignant cells into the body of the recipient (*36*).

Another approach has been to examine the use of alternate hydrogel cores (*2*, *37*), including those made of composite materials. Reinforcement of the alginate core through the formation of an interpenetrating network or composite may lead to improved mechanical properties while maintaining most of the desirable properties of Alg.

A number of alginate composite materials have been explored for cell encapsulation (*38*). Compounds added to the alginate forming the bead core were designed to be thermally (agarose (*39*)), ionically (carrageenan (*40*)) or photochemically gelled (*41*), designed to modify viscosity or water content (carboxymethylcellulose (*42*)), act as wall forming materials (cellulose sulphate (*43*), heparin (*42*)), control permeability or provide an improved environment for cell growth (chitlac - lactitol-functionalized chitosan (*44*)). Childs and coworkers formed a composite capsule composed of alginate and poly(sodium acrylate-*co*-N-vinylpyrrolidone) formed by photo polymerization of monomers allowed to diffuse into the CaAlg beads (*31*).

We recently described a pair of polyelectrolytes bearing complementary reactive groups that underwent spontaneous mutual cross-linking to produce a covalently cross-linked polyelectrolyte shell on CaAlg beads (*45*). In contrast to photochemical cross-linking approaches, this cross-linking reaction is based on condensation reactions that occur instantly upon contact. The resulting coated alginate capsules showed enhanced resistance to mechanical and chemical stress, attributed to the cross-linked outer coat. The improvements were however limited, and there was evidence of fibrotic overcoats after implantation, indicating an adverse immune reaction. Analogous four-layer shells, that included outer layers of PLL and alginate, led to improved biocompatibility, and further enhanced mechanical properties (*46*). Recently we investigated amine-bearing polyacrylate as possible replacements for PLL in the preparation of capsules for cell encapsulation. One of the synthetic polycations, poly(N-(3-aminopropyl)methacrylamide) (PAPM), was found to be a promising alternative to PLL (*47*).

We also used reactive polyelectrolytes to reinforce the core of CaAlg capsules. This process involves adding the reactive polyanion to the original alginate solution such that it first becomes trapped in the CaAlg core, and subsequently cross-linked by in-diffusion of PLL of suitable MW (*48*).

This process allows further control over wall thickness and location, compared to the usual sequential layer-by-layer deposition of polyelectrolytes. In one scenario, larger PLL chains (MW $\geq$ 15-30k) should lead to covalently cross-linked analogs to the conventional APA capsules, as these PLL chains may not penetrate deeply into the CaAlg bead. The second scenario, involving smaller PLL chains (MW < 15k) should lead to covalently core-cross linked capsules, for

In Polymeric Delivery of Therapeutics; Morgan, S., et al.;
ACS Symposium Series; American Chemical Society: Washington, DC, 2010.

which loss of alginate due to calcium-sodium exchange or oxidative breakdown (*49*) would be less critical. A third scenario, sequential exposure of the composite beads to high and low MW PLL, may permit separate control over shell and core cross-linking. In all cases the beads would receive a final coat of alginate, or the reactive polyanions (Scheme 1), in order to react surficial excess of polycation, and present an anionic surface to the host.

The first part of this chapter reviews the synthesis and characterization of cationic copolymers composed of methacryloyloxyethyl trimethyl ammonium hydrochloride and aminoethyl methacrylate, and the homopolymer of N-(3-aminopropyl)methacrylamide hydrochloride (APM), as well as reactive anionic copolymers composed of methacrylic acid sodium salts with methacryloyloxy ethyl acetoacetate. This part also describes their assembly and covalent crosslinking in the outer shell of CaAlg capsules. The second part concentrates on the core reinforcement process by the formation of covalent cross-linked networks throughout the core and/or shell of CaAlg capsules. Also, the morphology, mechanical strength and permeability of the capsules, the viability of encapsulated cells and the compatibility of the capsules with a murine host will be discussed in some detail.

Experimental

Materials

The syntheses of cationic copolymer p(MOETAC-*co*-AEM.HCl), C70 (70/30 mol ratio copolymer of [2-(methacryloyloxy)ethyl] trimethyl ammonium hydrochloride and 2-aminoethyl methacrylate) (*45*), its FITC analogs C70*f* (*45*), anionic copolymer p(MAANa-*co*-MOEAA), A70 (70/30 mol ratio copolymer of sodium methacrylate and 2-[methacryloyloxy]ethyl acetoacetate) of variable molecular weight (*48*), and its FITC analogs A70*f*, were described elsewhere (*45*, *48*).

The analogous A60 (THF, yield: 71%) and A50 (1:1 THF/ethanol, yield: 85%) were prepared by free radical polymerization in a similar fashion to A70 (*48*) except for the use of the polymerization solvents shown in brackets. Preparations of poly(sodium methacrylate) A100 (*45*), its FITC analog A100*f* (*48*), poly(2-aminoethyl methacrylate) C0 (*47*), poly(2-(methacryloyloxy)ethyl]trimethyl ammonium hydrochloride) C100 (*45*), poly(N-(3-aminopropyl)methacrylamide hydro chloride) PAPM (*47*), and Rhodamine labelled poly-L-lysine (PLL*r*) (*48*) have been described elsewhere in detail.

Instrumentation

The composition of A70, A60 and A50 was determined by ^{1}H NMR spectroscopy in DMSO-d6 using a Bruker AV 200 spectrometer. The composition of C70, and the pKa values of all amine-based polycations were determined by potentiometric titration with 0.1M NaOH on a PC titrate automatic titrator (Man Tech Associates). The degree of labelling with FITC and Rhodamine was

measured on a Varian Cary 50 BIO UV-Vis spectrophotometer. Gel permeation chromatography (GPC) analyses were performed at a nominal flow rate of 0.8 mL/min. The columns were maintained at 35°C and the system was calibrated with commercially available narrow dispersed molecular weight polyethylene glycol (PEG) standards (Waters, Mississauga, ON). The GPC system consisted of a Waters 515 HPLC pump, Waters 717 plus Autosampler, three Ultrahydrogel columns (0-3 kDa, 0-50 kDa, 2-300 kDa), and a Waters 2414 refractive index detector. Dextran-FITC samples were eluted with 0.1 M $NaNO_3$, while for A100, A100*f*,A70, A60 and A50, the mobile phase was 0.3 M $NaNO_3$ in 0.05M phosphate buffer (pH 7). All polyanions were prepared for GPC analysis by the addition of a stoichiometric amount of 1M NaOH to the acid-form precursor polymer, followed by dilution with the mobile phase. An Ubbelohde viscometer (viscometer constant: 0.00314 cSt/s), was used to determine MWs of all polycations dissolves in 1M NaCl at 20 ± 0.1°C. Prior to the measurements, all stock solutions were filtered through a 0.45 μm membrane filter.

Optical microscope images of polyelectrolyte complexes, and capsules were taken using an Olympus BX-51 optical microscope fitted with a Q-Imaging Retiga EXi digital camera and Image Pro software. Phase contrast microscope images were taken using a Wild M40 microscope. A Confocal laser scanning imaging system equipped with air-cooled Argon and HeNe lasers (LASOS; LGK 7628-1) and a ZEISS LSM 510 microscope using LSM Image browser software (version 3.5), was used to study the distribution of FITC and Rhodamine-labeled polymers in the capsules

Preparation of Ca Alg and Ca(A/A70) Beads

The CaAlg and Ca(A/A70) composite beads were prepared using an approach described by Ross et al. (*50*) Briefly, to prepare a Ca(A/A70) composite beads, aqueous solutions of 1.5 wt% Na alginate and 0.5 wt% A70 or A70*f* at pH 7 were filtered through sterile 0.45 μm Acrodisc syringe filters (Pall Corporation, USA). A modified syringe pump (Rassel Mechanical Inc. pump, model # A-99) was used to extrude the Alg-A70 mixture at a rate of 30.1 mL/hr through a 27-gauge blunt needle (Popper & Sons, New York), with a concentric airflow (4 L/min) passing by the needle tip to induce droplet formation. The droplets were collected in a 1.1 wt% calcium chloride, 0.45 wt% sodium chloride gelling bath (10x Alg-A70 volume) causing the formation of Ca(A/A70) composite beads. Twenty minutes after bead formation was complete, the supernatant was removed, and the resulting concentrated Ca(A/A70) composite bead suspension was washed in sequence with four-fold volumes of a) 1.1 wt% $CaCl_2$, 0.45 wt% NaCl for 2 minutes; b) 0.55 wt% $CaCl_2$, 0.68 wt% NaCl for 2 minutes; c) 0.28 wt% $CaCl_2$, 0.78 wt% NaCl for 2 minutes; d) 0.1 wt% CHES, 1.1 wt% $CaCl_2$, 0.45 wt% NaCl for 3 minutes.; and then e) 0.9 wt% NaCl for 2 minutes and stored in saline.

Analogous cell-containing composite beads were prepared by preparing a core solution containing 1.5 wt% sodium alginate, 0.5 wt% A70, and 2 million C_2C_{12} cells per mL of saline. This suspension was extruded to form beads as described above, except for the use of an Orion sage pump, model # M362 located in a sterile laminar flow hood, and a liquid flow rate of 99.9 mL/hour. The cell containing

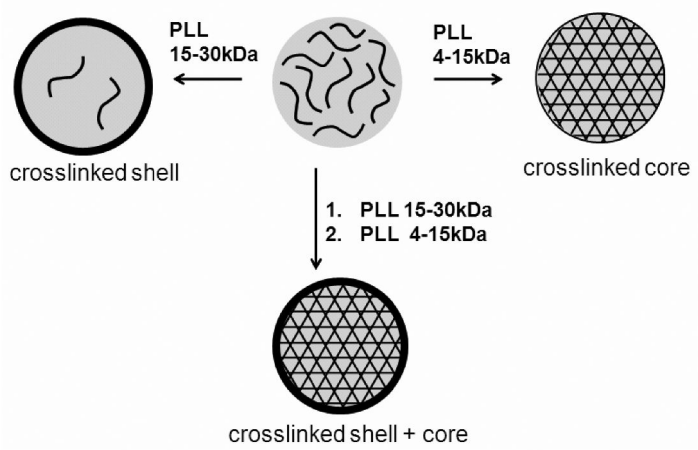

Scheme 1. Schematic representation of the capsule morphologies formed when embedding reactive polyanion within the CaAlg capsule, followed by reaction with high MW PLL, low MW PLL, and sequentially with high and low MW PLL.

capsules were washed as above, and stored in serum free media at 4°C for further use.

The corresponding CaAlg beads were prepared as described above, without adding A70 to the extruding mixture.

Encapsulation Procedure

APA control capsules were prepared by successive exposure to PLL followed by Alg as described elsewhere (*51*). For the 2-layer capsules, CaAlg beads were coated with 0.5 wt% C70 and 0.5 wt% A70 for 10 min each. For 4-layer capsules, the resulting CaAlg-C70-A70 capsules were coated with 0.05 wt% PLL for 6 min, and then with 0.03 wt% Alg for 4 min. Each layering step was followed by sequential washes described elsewhere (*45*, *46*). For some 2-layer capsules, C70 was replaced by PAPM or PLL for comparison. For composite capsules, Ca(A/A70) composite beads were exposed to 0.05 or 0.5 wt% PLL (pH = 8, saline) for 6 minutes, followed by sequential washes (*45*, *46*) and then coated with 0.03 wt% Alg for 4 minutes, followed by three washes with 0.9 wt% NaCl. After the final washing step, in each case the cell containing capsules were cultured in serum free media in a tissue culture incubator at 37°C, while empty capsules were stored in normal saline.

Microcapsules Properties

The chemical and mechanical stress tests for capsule integrity (*47*), the protein (bovine serum albumin) uptake by capsules (*47*), and permeability studies (*48*) were described elsewhere.

In Polymeric Delivery of Therapeutics; Morgan, S., et al.;
ACS Symposium Series; American Chemical Society: Washington, DC, 2010.

C_2C_{12} myoblast cells from the American Type Culture Collection [ATCC] were cultured and encapsulated, and the *in vitro* and *in vivo* cell viabilities measured as described in the literature (*45*).

Mechanical Stabilities

The mechanical properties of individual capsules were measured using a micro compression tester. Single capsules were compressed between a 4 mm^2 silicon wafer attached to a piezo-electric transducer, and a glass microscopy slide mounted on an inverse microscope. The wafer was positioned over one capsule at a time and moved down vertically at a constant speed of 10 μm/s with the help of a stepper motor while plotting the force registered against vertical displacement. Compression data were corrected both for the buoyancy of the silicon wafer, and for the elastic give of the experimental set up. The experiments were performed at room temperature (23 ± 2 °C).

Results and Discussion

The aim of this chapter is to use the oppositely charged reactive polyelectrolytes developed in our lab to strengthen CaAlg beads by the formation of cross-linked interpenetrating networks at the outer shell or throughout the core, and to compare their properties with the conventional APA capsules.

Synthesis of Polyelectrolytes

The synthetic polyelectrolytes were prepared by conventional free radical polymerization. The structure and properties of the natural and synthetic polyelectrolytes used in this research are described in Scheme 2 and Table 1. The composition of copolymers was measured by either titration or ^1H NMR, and found to closely match the feed ratio of the two monomers. Typically, monomer to initiator ratios of 50:1 and 100:1 were used for both polycations and polyanions. However, to obtain polyanions (A70) with number average MWs of 22, 42 and 149k, respectively, monomer to initiator ratios of 20:1, 100:1 and 800:1 were used. Attempts to prepare higher MW of A70 resulted in gellation, attributed to covalent cross-linking during polymerization.

Fluorescently labelled versions of the polymers were prepared by reaction with FITC (A70*f*, C70*f*) or via copolymerization with fluorescein O-methacrylate (A100*f*). The final label contents were determined by UV/Vis spectroscopy, with C70*f*, A70*f*-22k, A70*f*-42k, A70*f*-149k, and A100*f* found to have 1.7, 0.22, 0.34, 0.32, and 0.42 mol% of the total monomer units labelled with fluorescein. Unless specifically noted, A70 or A70*f* with a MW of 42k was employed throughout the research. PLL having MWs of 1-4k, 4-15k, and 15-30k were similarly labelled by reaction with rhodamine B isothiocyanate (PLL*r*), leading to label contents of 0.76, 0.77 and 0.62 mol%, respectively.

In Polymeric Delivery of Therapeutics; Morgan, S., et al.;
ACS Symposium Series; American Chemical Society: Washington, DC, 2010.

Physical State of the Polyelectrolyte Complexes (PECs)

Initial model experiments were carried out to understand the interaction between polycations and polyanions, and $CaCl_2$ used in this study.

CaAlg is a solid gel with significant mechanical strength. CaA100, obtained by mixing a 1 wt% solution of A100 with excess 100 mM $CaCl_2$, as well as CaA90 and CaA80 formed liquid coacervate complexes (images not shown), reflecting weaker interactions of Ca^{2+} with these polyanions. CaA70 (22, 42 or 149k), CaA60 and CaA50 showed no macroscopic phase separation, likely due to the lower carboxylate content of these polymers, indicating that these polyanions should retain some mobility even within the CaAlg beads.

Polyelectrolyte complexation between oppositely charged polyanions (Alg, A100, A70) and polycations (PLL, C0, C70, C100, PAPM) at 1 wt% total polymer concentration and pH 7 all gave phase-separated solids. Ionic polyelectrolyte complexes (PECs) formed with the non-reactive analogs, C100 and A100, were shown earlier to dissolve when exposed to [NaCl] > ~500 mM (*52*). In contrast, the solid PECs between primary amine-containing polymers and A70 only swelled upon exposure to 2M NaCl, but did not dissolve (Figure 1), reflecting the presence of covalent cross-links. Formation of such cross-linked complexes throughout or at the surface of CaAlg capsules should lead to capsules better able to resist environmental stresses compared to purely ionic polyelectrolyte complexes.

A model study was also undertaken to further probe the nature and strength of the interactions between the nonreactive polycation, C100 and polyanion, A100 in presence of gelling (Ca^{2+}) and non-gelling (Na^{+}) ions. It was found that increasing the non-gelling ion (Na^{+}) changes the solid PEC first into a liquid, and above 350 mM, into soluble species. In contrast, addition of gelling ion (Ca^{2+}) causes displacement of the C100 from the complex, until at $[CaCl_2] \geq 100$ mM the liquid complex consists of almost exclusively CaA100, with only traces of C100 detectable by ^{1}H NMR (data not shown).

Two-Layer (A-C70-A70) Microcapsules

CaAlg beads as used for cell encapsulation consist of highly hydrated alginate networks that are ionically cross-linked mainly through their guluronic acid residues. Exposure to aqueous solutions of PLL or other polycations, followed by exposure to a biocompatible polyanion, usually alginate, has been a common approach to improve strength as well as permeability control of CaAlg beads containing live cells. Failure modes in long-term implantation may include calcium loss to the host, immune or inflammatory response of the host to the encapsulated cells or to the alginate, loss of polyelectrolytes coating, and/or mechanical degradation.

We have investigated the feasibility of using the synthetic polyelectrolytes C70 and A70 to replace the conventional PLL and outer alginate, respectively, for the preparation of stronger capsules. The key to this approach is that the cross-links are formed between complementary reactive groups that are attached to two different polyelectrolytes. The polycation and polyanion bear amino and acetoacetate groups, respectively, that undergo *in situ* covalent cross-linking

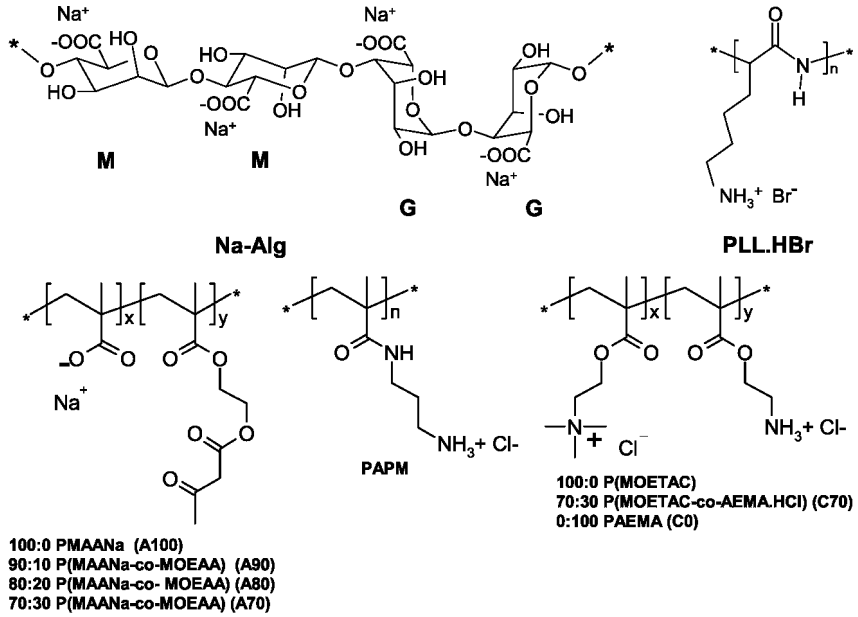

Scheme 2. Natural and Synthetic Polyelectrolytes Used in this research

reaction once the polyelectrolytes are brought into close proximity by electrostatic interactions, as shown in Scheme 3. The reactive groups are polymer-bound, and their respective polyelectrolyte backbones are designed to reduce their bioavailability and hence their toxicity towards both encapsulated cells and host. Sequential coating of CaAlg beads with these polyelectrolytes (Scheme 3) should lead to a permanently cross-linked skin that may strengthen the capsules, yet have good biocompatibility and permeability.

Narrow-disperse CaAlg beads were first prepared by extruding a 1.5 wt% Na alginate solution, optionally containing C_2C_{12} mouse cells, into a 1.1 wt% $CaCl_2$, NaCl gelling bath. Following a standard washing procedure, these CaAlg beads ("A") were exposed, in sequence, to dilute solutions of the polycation, C70 and the polyanion, A70 to produce AC70A70 capsules. Uncoated CaAlg beads are stiff gels at physiological salt concentrations. Upon treatment with 5 wt% (170 mM) Na citrate to extract the calcium, the beads swell and become almost transparent and difficult to see. In contrast, when the AC70A70 (Figure 2a) and the control APA capsules were exposed to 170 mM Na citrate, the cores of the capsules dissolved, while the shells survived. Subsequent exposure to 2M NaCl completely dissolved the APA control capsules, while the shell of the AC70A70 capsules remained intact (Figure 2b). This indicates that APA shells are held together by ionic bonds that dissociate at high ionic strength, while the AC70A70 capsules have a covalently cross-linked shell that survives at high ionic strength.

Fluorescently labelled AC70A70-type capsules, prepared using either FITC-labelled C70 (designated C70*f*) or A70 (designated A70*f*), show shell thicknesses of up to 35 micron in confocal laser scanning microscopy (CLSM) images (Figure 2c). Shell thicknesses vary with MW of PLL and exposure time, in agreement with

In Polymeric Delivery of Therapeutics; Morgan, S., et al.;
ACS Symposium Series; American Chemical Society: Washington, DC, 2010.

Table 1. Polyelectrolyte Properties

Polyelectrolyte	*Composition*	*M_n (kDa)/PDI*
Na-Alg	G/M, 40:60[a]	428[d]
PLL	-	1-4, 4-15, 15-30[a]
PAPM	-	260[e]
C100	-	300[e]
C70	MOETAC/AEMA, 70:30 (±4)[b]	167[e]
C0	-	299[e]
A100	-	5.4[a]
A100-38k	-	38/2.6[f]
A100f	-	29 / 2.8[f]
A90	MAA/MOEAA, 89:11[c]	29/1.7[f]
A80	MAA/MOEAA, 79:21[c]	41/2.0[f]
A70-22k	MAA/MOEAA, 70:30 (±3)[c]	22/ 3.1[f]
A70-42k	MAA/MOEAA, 70:30 (±3)[c]	42 / 2.4[f]
A70-149k	MAA/MOEAA, 70:30 (±5)[c]	149/ 1.7[f]
A60	MAA/MOEAA, 64:36[c]	32/2.3[f]
A50	MAA/MOEAA, 44:56[c]	31/2.4[f]

[a] Given by supplier. [b] Copolymer composition in mol% determined by titration. [c] Copolymer composition in mol% determined by ^{1}H NMR. [d] See ref (*31*) [e] M_w obtained from viscometry data. [f] M_n and polydispersity index (PDI) determined by GPC.

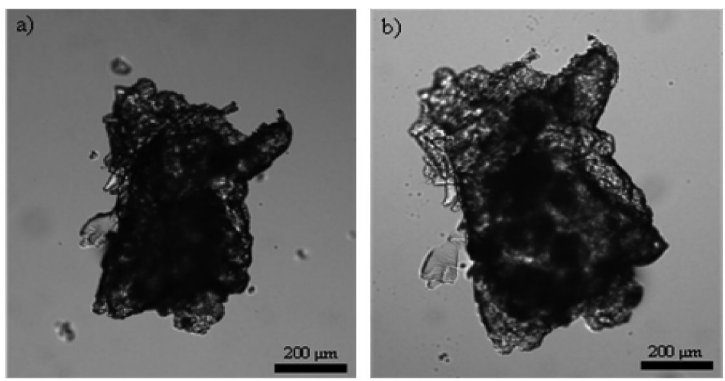

Figure 1. OM image of a piece of self-cross linked polyelectrolyte complex of C70/A70 a) in saline; and b) after exposure to 2M NaCl for 20 minutes.

recent analogous studies (*53*). Layers of similar thickness are observed regardless of which polyelectrolyte is labelled, indicating the presence of a homogeneous

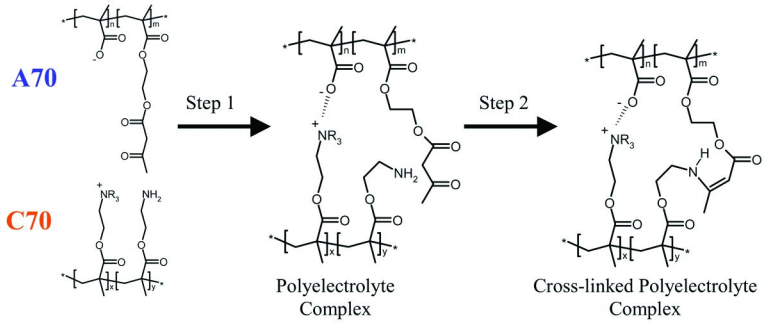

Scheme 3. Reactive copolymers [C70(amino); A70(acetoacetate)] for in-situ cross-linking for the formation of cross linked shell/core in CaAlg beads.

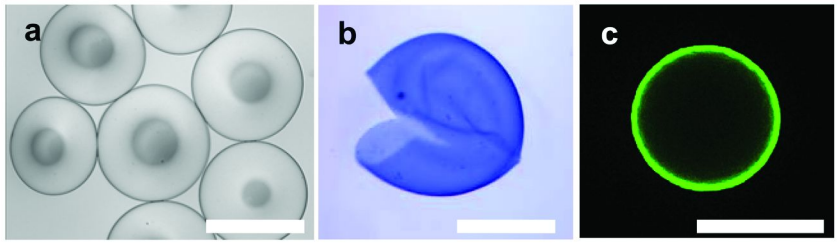

Figure 2. OM image of a) AC70A70 microcapsules, b) Trypan Blue stained shell remaining after exposure to 170 mM citrate and 2M NaCl (cut open to reveal capsular nature), c) CLSM image from the equatorial region of a AC70fA70f microcapsules). Scale bar 500 μm.

mixture of the two polyelectrolytes C70*f* and A70*f* at the surface of the CaAlg bead.

CaAlg beads bearing these cross-linked shells demonstrated greater resistance to osmotic pressure changes compared to conventional beads coated with PLL and Alg (APA). Permeability of such cross-linked hydrogel membranes was studied by GPC analysis of different MWs of poly(ethylene glycol) (PEG) diffusing through analogous flat model membranes. Both APA and AC70A70 membranes were found to have MW cut-offs between 150 kDa and 200 kDa, suitable for exclusion of immuno-related proteins (*54*).

Figure 3 shows a phase contrast microscope image of C_2C_{12} cells encapsulated in APA and AC70A70 capsules, after incubation for one week. Cell viability in *in-vitro* studies of AC70A70 capsules was found to be slightly lower than in the control APA capsules, but the number of live cells remained stable, and the cells were replicating with extended incubation. Preliminary studies of *in vivo* cell viability, after implantation of cross-linked AC70A70 capsules in mice for 1 to 2 weeks, showed fibroid over-coating of many capsules (Figure 4b). This over-coating indicates an immune response of the host that would limit viability of the encapsulated cells. The next section describes one approach to reducing this immune response.

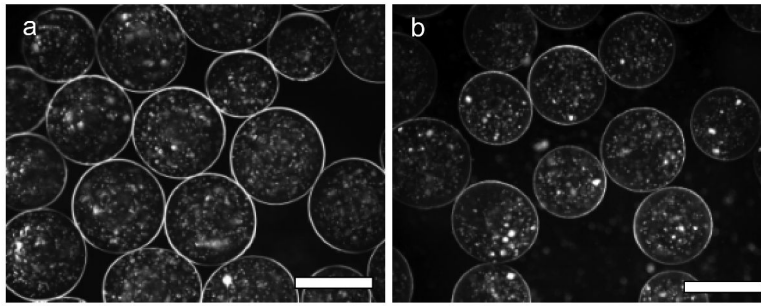

Figure 3. Phase contrast microscope image of C_2C_{12} cells encapsulated in a) APA, b) AC70A70 after incubation for 1 week. Coating conditions: PLL (0.05% w/v in saline, 6 min); Alg (0.03% w/v, 4 min), C70 (0.5% w/v, 10 min), A70 (0.5% w/v, 10 min). Scale bar 500 μm.

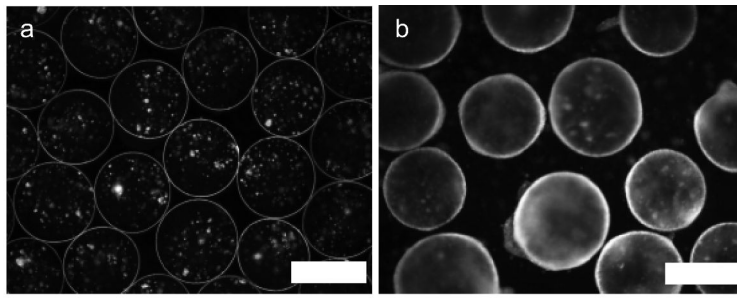

Figure 4. Phase contrast microscope image of C_2C_{12} cells encapsulated in a) APA, b) AC70A70 retrieved from mice after implantation for 1 week. Scale bar 500 μm.

Four-Layer (A-C70-A70-PLL-Alg) Microcapsules

We realized from the above *in vivo* study of 2-layer capsules in mouse models that there is an immune reaction of the host to the capsules or encapsulated cells after implantation. As analogous cell-containing APA capsules prepared from the same alginate do not show this immune reaction, we suspected that C70 and/or A70 might be responsible, by binding components of the BSA-based culture medium used for incubation. To address this issue, we decided to try to hide the C70/ A70 outer layer by additional exposure to PLL followed by Alg, leading to a 4-layer capsule denoted A-C70-A70-PLL-Alg.

The 4-layer capsules show slightly poorer cell viability, which is attributed to the encapsulation process itself. The number of live cells remained stable, and begins to increase shortly after encapsulation. We studied the immune stimulating effect (fibroid overgrowth) of these 4-layer capsules by varying the concentration and compositions of polyelectrolytes, and changing the medium. Binding of FITC labelled BSA (BSA*f*) to the 4-layer capsules was studied by CLSM, as shown in Figure 5. It was found that presence of C70 strongly correlates with protein binding near the capsules surface, while A70 had a lesser effect. Reducing

In Polymeric Delivery of Therapeutics; Morgan, S., et al.;
ACS Symposium Series; American Chemical Society: Washington, DC, 2010.

the concentration of C70 and A70 also reduced BSA*f* binding (data not shown). Using serum free medium instead of regular medium to culture the capsules post fabrication eliminates this host reaction. The APA and 4-layer capsules were cultured in serum free media before implantation into the peritoneal cavity of mice, and retrieved after 1 week is shown in Figure 6. The 4-layer capsules are more resistant to the chemical and mechanical stress tests than control APA capsules. The permeability of 4-layer capsules was determined by CLSM and GPC using BSA*f* and narrow dispersed PEGs of different MW. The MW cut-off of the 4-layer capsules was shown to be similar to that of the control APA capsules, and suitable for cell encapsulation. *In vitro* and *in vivo* viability of encapsulated cells of 4-layer capsules was similar to that of APA capsules.

Polycations for Alginate Microcapsules

In our experiments, capsules containing C70 have shown significant undesirable protein binding. In addition, C70 coated capsules are more prone to aggregation during the coating process than PLL coated capsules, and preliminary studies show that primary amine containing methacrylic ester can undergo intra and/or intermolecular amidation in aqueous solution over time that leads to cross-linked gels and interferes with capsule coating. We hence explored other polycations (Scheme 2, Table 1) as possible replacements for C70. Such polyamines should ideally be inexpensive, non-cytotoxic, not elicit protein-binding or a strong host reponse, yet engage in cross-linking with polyelectrophiles such as A70. We synthesized poly(aminopropylmeth acrylamide), (PAPM) and poly(aminoethylmethacrylate) (C0) by free radical polymerization, and compared them with C70 and PLL in the preparation of A-polyamine-A70 capsules for cell encapsulation. CaAlg beads were coated with the four different polycations (C70, C0, PAPM, and PLL), using concentrations from 0.01-0.5 wt% in saline at pH 7.5. The PLL coated capsules were well dispersed for all polycation concentrations. In contrast, CaAlg beads exposed to C70 or C0 in saline, aggregated at polycation concentrations from 0.01 to 0.1 wt%, but stayed dispersed at 0.5 wt%, and CaAlg beads exposed to PAPM in saline aggregated at all PAPM concentrations examined (0.01-0.5 wt%). Using PAPM solutions in 1.1 wt% $CaCl_2$ and 0.45 wt% NaCl solution, a mixture commonly used for the gelling bath, prevented this aggregation during coating. After polycation coating, the beads were coated with A70 in saline, to give capsules with a covalently cross-linked shell, that survive the challenge with citrate and high ionic strength. The representative optical microscopy images of shell cross-linked capsules are shown in Figure 7.

The resulting capsules were then tested for mechanical strength, viability of encapsulated cells and host immune response. These results showed that PAPM is comparable to PLL in terms of shell strength, cell viability and protein binding, in shell cross-linked CaAlg capsules formed with the reactive polyanion A70. They also show better capsule strengths compared to C0 and C70. It was also shown that PAPM as well as PLL are protected from the undesirable intra/intermolecular amidation reactions during storage that were seen for C70 and for C0. In

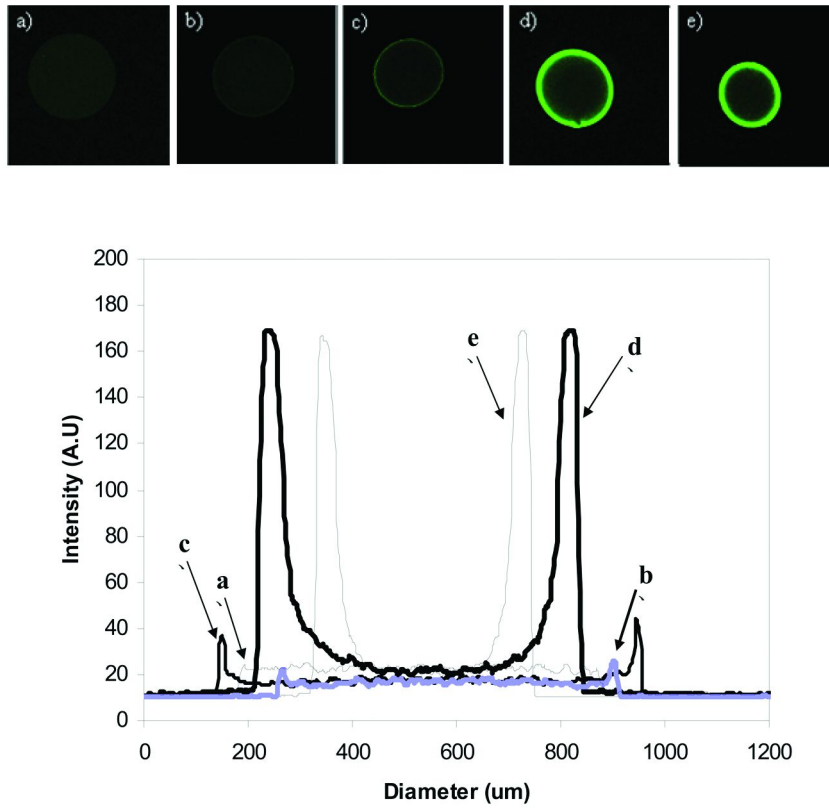

Figure 5. Top – CLSM images, bottom – line profile of a) APA, b) APA100PA, c) APA70PA, d) AC70A100PA and e) 4-layer (AC70A70PA) microcapsules exposed in 0.05 w/v% BSA-FITC at 20 °C for 24 h.

addition, PAPM offers the advantage of controlled MW using controlled radical polymerization techniques, and easy access to copolymers incorporating some of the wide range of acrylic monomers available.

Composite Microcapsules

This work explores the feasibility of using synthetic polyelectrolytes to form cross-linked networks throughout the CaAlg bead, leading to formation of a permanent three-dimensional support structure for cell transplantation and other uses.

This approach involves adding the synthetic reactive polyanion, A70, with the initial Na Alg solution. The resulting Ca(Alg/A70) beads are then covalently crosslinked by exposure to PLL solutions in saline, to form a covalently cross-linked A70-PLL network within the Ca(Alg/A70) composite hydrogel, with morphologies dependent on the MWs and mobilities of the two polyelectrolytes used.

It was found that 15-30k PLL did not penetrate the CaAlg gel matrix past the outer 35 micron (*45*, *46*, *55*) resulting in a shell crosslinked structure similar to that found in the layer-by-layer capsules discussed above (*45*, *46*). On the other hand, 4-15k PLL was able to diffuse in the present Ca(Alg/A70) beads, resulting in core-cross linked networks.

The MW and hence the mobility of the A70 was similarly shown to have significant effects, with higher MW A70 being more efficiently retained in the composite beads.

(A/A70) PA Composite Microcapsules

Ca(A/A70) beads were prepared by dripping saline solutions containing 1.5 wt% Na alginate and 0.5 wt% polyanion A70 (or its fluorescently-labelled analog, A70*f*), adjusted to pH 7, into a $CaCl_2$, NaCl gelling bath (*56*). The composite beads formed had an average diameter of 650 μm and appeared identical to those formed using alginate alone (Figure 8). The beads were subsequently exposed to different concentrations of PLL having different MW, to form shell-crosslinked, and core-crosslinked composite capsules respectively.

Shell-Cross Linked (A/A70)PA Microcapsules

Ca(A/A70) beads exposed to 0.05 wt% PLL (15-30k), washed with saline and then coated with a 0.03 wt% Na alginate solution looked similar to the uncoated beads but the surface was evenly stained by trypan blue indicating the presence of a continuous polycation layer (image not shown). In addition, the surface appeared pink when rhodamine labelled PLL (PLL*r*) was used to coat the composite beads.

The composite bead preparation was repeated with A70*f*, in order to demonstrate the inclusion of the synthetic polyanion and to probe its distribution within the bead. Following bead preparation, the $CaCl_2$ gelling bath and the washing solutions were analyzed by UV-Vis spectroscopy, and showed that 60 ± 5% of the original A70*f*-22k or A70*f*-42k, and 40 ± 5% of the corresponding higher MW A70*f*-149k were lost from the beads, predominantly to the gelling bath (Figure 9). No additional A70*f* loss was observed during the subsequent PLL coating process. Uncoated Ca(A/A70*f*) beads stored in a 6-fold excess of saline at 4 °C lost an additional 3% of the original A70*f* after 2 days, and 16% after 3 months. In contrast, (A/A70*f*)PA capsules did not lose a significant amount of A70*f* to the supernatant over 8 months of storage.

Thus, A70*f* is lost principally in the gellation step during which the droplets were also found to shrink to about 60% of their original volume, a value consistent with other studies (*57*, *58*). Use of higher MW A70 increases the retention of the polymer, possibly due to enhanced entanglement.

CLSM was used to demonstrate the distribution of A70*f* and PLL*r* within the capsules. After gelling in the $CaCl_2$ bath, A70*f* is initially homogeneously distributed within the Ca(A/A70*f*) beads (Figure 10a). Images obtained 1-2 hours after coating these Ca (A/A70*f*) beads with PLL and Alg (Figure 10b), show in

In Polymeric Delivery of Therapeutics; Morgan, S., et al.;
ACS Symposium Series; American Chemical Society: Washington, DC, 2010.

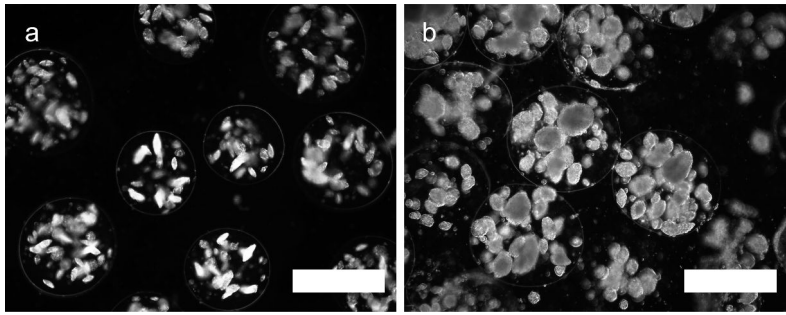

Figure 6. Phase contrast microscope image of C_2C_{12} cells encapsulated in a) APA, b) A-C70-A70-PLL-Alg retrieved from mice after implantation for 1 week. 4-layer-capsules cultured in serum-free medium for 72 hours before implantation. Scale bar is 500 µm.

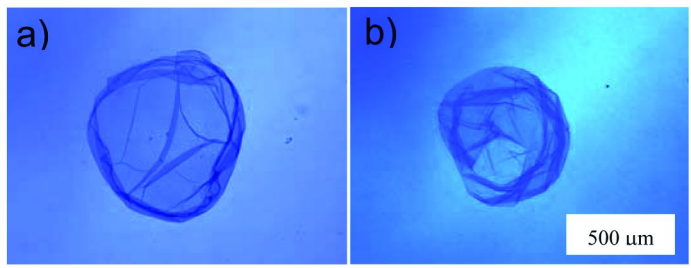

Figure 7. OM images of a) A-PAPM-A70 (0.5/0.5), and b) A-C0-A70 (0.5/0.5) cross-linked capsules shell. After treatment with 170 mM Na citrate and then 2 M NaCl, followed by trypan blue staining. Polycation/polyanion concentrations (wt %) are shown in brackets.

addition a very thin outer shell, perhaps the result of electrostatic or covalent capture of A70*f* by the PLL layer.

After 5 months storage uncoated beads showed considerable fluorescence in the supernatant. However, the retained A70*f* is homogeneously distributed within the capsule. These results suggest that a fraction of the A70*f* chains are short and hence mobile enough to diffuse out of the CaAlg gel, while the remainder are trapped within the gel. The CLSM image of 5-month-old coated capsules is similar to that seen just after preparation (Figure 10b). The A70*f* is retained in the capsules confirming that the PLL coating prevents the loss of A70*f*.

When the coated capsules were treated with excess 170 mM Na citrate for 18 hrs to liquefy the CaAlg core, the capsules swelled (40-50% diameter increase). Mechanical rupture released liquid from the core, indicating that the amount of PLL able to diffuse into the core was not sufficient to effect core crosslnking.Accordingly, Rhodamine-labelled versions of PLL (PLL*r*) of different MW were used to study the effect of PLL MW and concentration on core crosslinking.

CLSM images of capsules coated with 0.05 wt% solutions of PLL*r* show that higher MW PLL*r* (15-30k) remains concentrated near the capsule surface

In Polymeric Delivery of Therapeutics; Morgan, S., et al.;
ACS Symposium Series; American Chemical Society: Washington, DC, 2010.

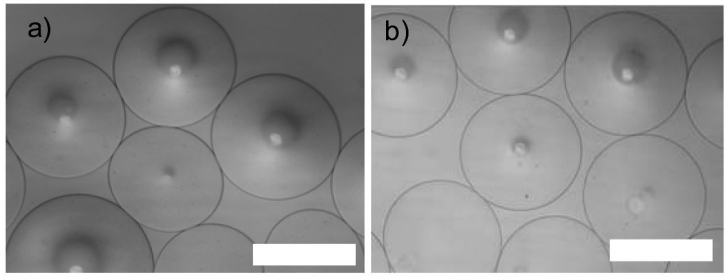

Figure 8. Optical microscope image of a) Ca Alg beads, b) Ca(Alg/A70f) composite beads. The scale bar is 500 μm.

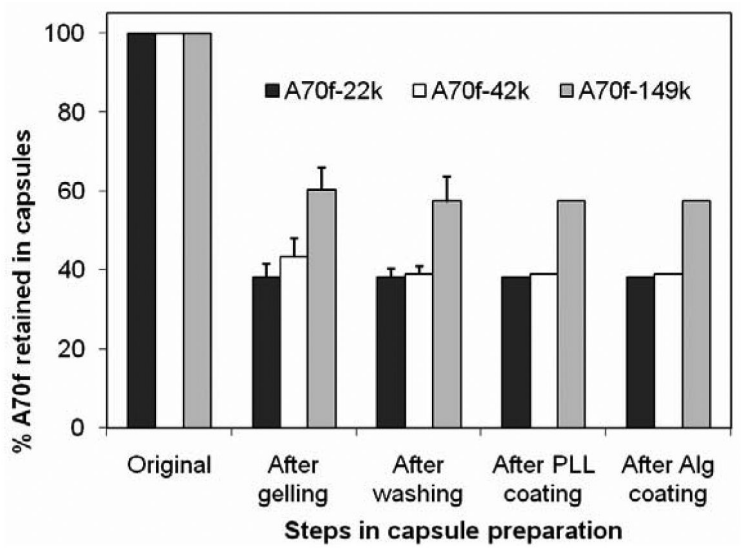

Figure 9. Percentage of A70f remaining in the composite microcapsules at different stages of the capsule preparation. Error bars show the standard deviation for select experiments performed in triplicate.

(Figure 11a). Weak fluorescence is seen in the capsule interior, indicating that a fraction of the PLL*r* is able to diffuse through the CaAlg gel. On the other hand, the lowest MW PLL*r* (1-4k) is evenly distributed throughout the composite capsules (Figure 11c). This is consistent with a number of earlier reports (*4*, *53*, *59–61*). The intermediate MW PLL*r* (4-15k) showed both formation of a distinct shell, and significant in-diffusion to the core of the bead (Figure 11b). The integrity of uncoated and PLL (0.05 wt%) coated Ca(A/A70) composite beads in the presence of Na citrate and NaCl was examined by optical microscopy and compared with that of control APA capsules. Uncoated beads composed of Ca(A/A70) or CaAlg are stable at physiological salt concentrations but dissolve when exposed to 170 mM Na citrate, which extracts the calcium from the gel. In contrast, addition of Na citrate to PLL(4-15k or 15-30k) coated capsules such as APA or Ca(A/A70)PA caused the core of the beads to dissolve, while the shells consisting

In Polymeric Delivery of Therapeutics; Morgan, S., et al.;
ACS Symposium Series; American Chemical Society: Washington, DC, 2010.

of the polyelectrolyte complex survived. However, upon addition of 2M NaCl while vigorously agitating, or 0.1M NaOH, the ionically cross-linked APA shells weakened or dissolved while the covalently cross-linked shells of the (A/A70)PA capsules remained intact.

Figure 12a shows a composite bead coated with 0.05 wt% PLL (4-15k). After sequential exposure to 170 mM Na citrate followed by 2M NaCl, the capsule shell was manually cut under the microscope with a micro knife (Figure 12b), revealing both a thin cross-linked shell due to reaction between the higher MW fraction of PLL, and the presence of mobile A70*f* diffusing out through the hole in the shell.The shell is self-supporting, but it is clear that the core of the bead is not cross-linked, likely due to the presence of insufficient amounts of PLL. The resulting capsules hence constitute shell cross-linked shell capsules, analogous to the shell-cross-linked capsules prepared earlier using sequential exposure of CaAlg beads to polycation and A70 (*45*, *46*), except that the reactive A70 is here supplied from the interior of the capsule. The outer surface of the capsule, after coating with alginate, then resembles the conventional APA capsules.

Figure 11c shows a composite bead coated with low MW PLL (1-4k, 0.05 wt%) in which PLL*r* homogeneously distributed throughout the beads. After exposure to Na citrate, the coated capsules dissolved within seconds. This indicates that although this low MW PLL readily penetrates the interior of the beads, at the present concentration of 0.05 wt% it is unable to crosslink the A70 to the extent necessary to give a crosslinked shell or core. The chains may be too short to effectively bridge between A70 and/or Alg chains.

Core-Cross Linked (A/A70)PA Microcapsules

Model experiments, based on combining small aliquots of aqueous solutions of A70 and PLL in different ratios, indicated that formation of cross linked macroscopic complexes required PLL to be present in stoichiometric or larger amounts, relative to A70. Use of sub-stoichiometric amounts of PLL resulted only in formation of turbid solutions, reflecting formation of PLL micro gels, likely coated with A70.

The results above indicated that (A/A70(42k) beads retain roughly 40% of their original loading of A70 or A70*f* at the point of exposure to PLL. These composite beads were exposed to appropriate volume of 0.05 wt% PLL, providing a near stoichiometric *overall* ratio of A70/PLL. However, UV/Vis analysis of a supernatant PLL*r*(15-30k) solution after coating showed that only half of this PLL was actually absorbed by the composite beads. In addition, most of the bound PLL (15-30k and 4-15k), forms a dense shell at the surface as indicated by Figure 11(a and b).

Analysis of the in-diffusion patterns (Figure 11) indicated that the intermediate MW PLL (4-15k) might represent a good compromise between ease of in-diffusion, and a MW high enough to crosslink the A70 in the core, provided it is available in sufficiently high concentration to compensate for incomplete capture and preferential binding to the shell.

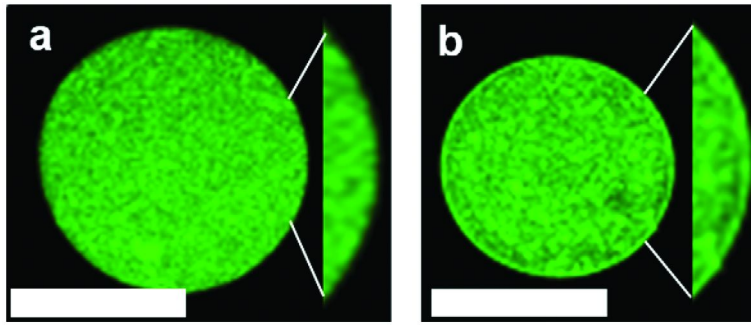

Figure 10. CLSM equatorial optical section of Ca(A/A70f) composite capsule: a) uncoated and b) coated with PLL (15-30 kDa) (0.05 wt%, 6 min) and then alginate (0.03 wt%, 4 min). The scale bar is 500 μm.

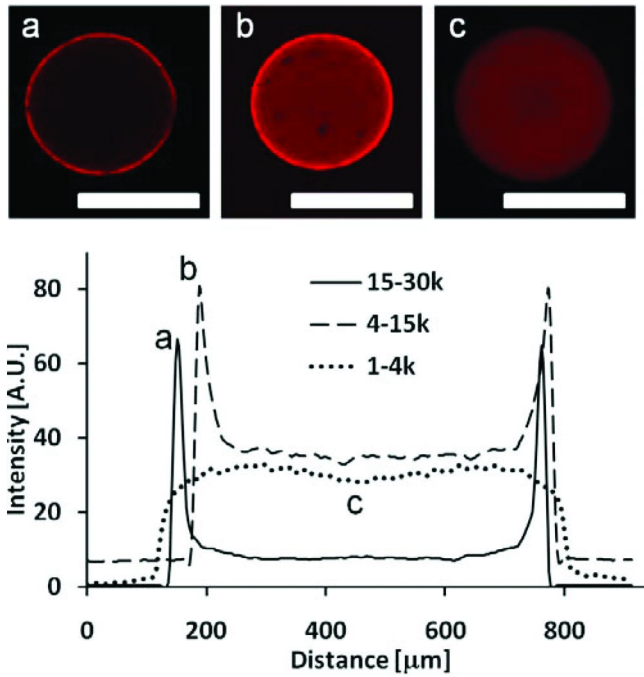

Figure 11. Top: CLSM equatorial optical sections of (A/A70)PA capsules made with PLLr of a) 15-30 kDa; b) 4-15 kDa; and c) 1-4 kDa. Bottom: 25 pixel wide line profiles taken from the images. Coating conditions: PLLr (0.05 wt% in saline, 6 min); Alg (0.03 wt%, 4 min).

Accordingly, we explored increasing the PLL (4-15k) concentration from 0.05 to 0.5 and 1 wt%. Coating using 1 wt% PLL solution resulted in wrinkling of the bead surface, while 0.5 wt% PLL (4-15k) resulted in smooth bead surfaces. Figure 13a shows (A/A70*f*)PA capsules coated with 0.5 wt% PLL (4-15k), followed by Alg (0.03 wt%). The resulting capsules were manually cut, and exposed to 70 mM

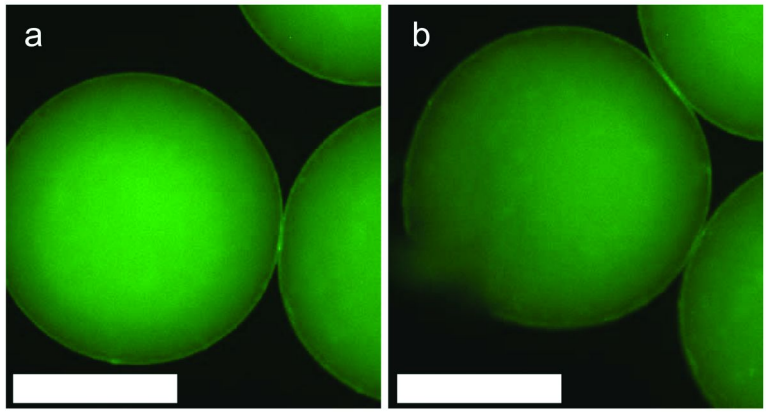

Figure 12. Fluorescence microscopy images of (A/A70f)P(4-15 kDa, 0.05 wt%) A(0.03 wt%) capsules; a) as formed, and b) after being exposed to citrate (170 mM) and NaCl (2 M), and manually cut with a micro-knife. Scale bar: 300 μm

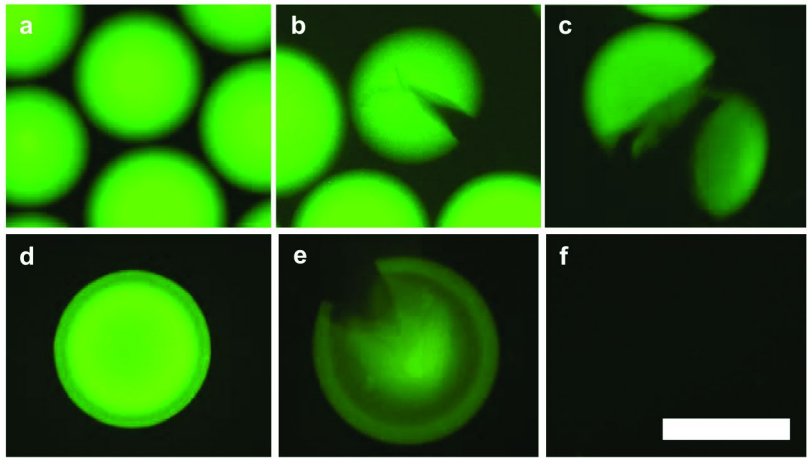

Figure 13. Fluorescence microscopy images of a) (A/A70f)P(4-15k, 0.5 wt%)A(0.03 wt%) and d) (A/A100f)P(4-15k, 0.5 wt%)A(0.03 wt%); e) the beads were manually cut, and then exposed to excess 70 mM Na citrate; c, f) after further treatment with 2 M NaCl. The scale bar is 500 μm.

Na citrate (*62*) (Figure 13b) and then 2M NaCl (Figure 13c). The capsules undergo little swelling and there is minimal loss of A70*f* demonstrating that sufficient PLL has diffused into the core to crosslink the bead throughout. The crosslinked beads also survived subsequent treatment with 0.1M NaOH (not shown).

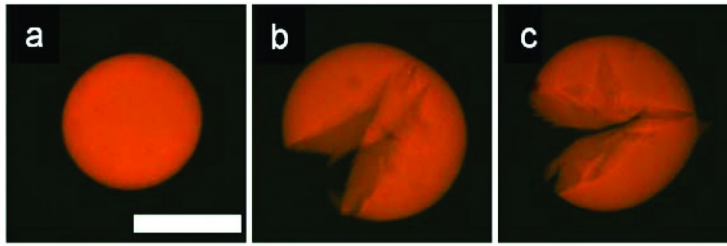

Figure 14. Fluorescence microscopy images of core-cross linked (A/A70)PLLr (4-15k, 0.5 wt%)A (0.03 wt%) composite capsules to show the location of PLLr (4-15 kDa). a) As formed; b) after addition of excess 70 mM Na citrate and crushing; c) following addition of excess 2 M NaCl. The scale bar is 500 μm.

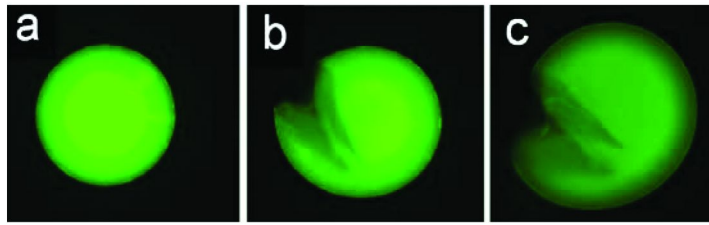

Figure 15. Fluorescence microscopy images of (A/A70f)PA microcapsule prepared by exposure to both high and medium MW PLL. Ca(A/A70f) composite beads were coated with 0.05 wt% PLL (15-30k) (1 min), and then with 0.5 wt% PLL (4-15k) (6 min), followed by 0.03 wt% Alg (4 min). a. As formed, b. After challenge with excess citrate and manual cutting. c. After exposure to excess 2 M NaCl. The scale bar is 300 μm.

Capsules formed using A100*f* (38k) instead of A70*f* (42k) confirmed the role of covalent crosslinking. Figure 13d shows the fluorescence optical microscope image of a (A/A100*f*)P(4-15k, 0.5%)A(0.03%) capsule. Exposure of these capsules to 70 mM Na citrate for about 5 minutes resulted in swelling of the outer layer. Manual cutting confirmed the presence of a swellable shell (Figure 13e) and shows an inner core. Subsequent exposure to 2M NaCl completely dissolved both shell and core within three minutes (Figure 13f), confirming that the permanent structure shown in Figure 13(a-c) is indeed based on covalent cross-linking.

To map the distribution of PLL, Ca(A/A70) composite beads were coated with rhodamine-labelled PLL*r* (4-15k) and examined by fluorescence microscopy (Figure 14). Figures 14a shows an intact capsule, while 14b and c show capsules that were exposed to excess 70 mM Na citrate and then manually crushed, followed by the addition of 2M NaCl revealing both shell and core cross-linking. The presence of a distinct PLL*r* shell in addition to core cross-linking suggests that the higher MW fraction of PLL*r*(4-15k) forms a surface network, while the lower MW fraction diffuses into the core to cross-link with A70. To test if core and shell could be separately crosslinked, CaAlg beads were coated sequentially with two PLL solutions having different MWs, a variation of the approach described

by Prokop et al (*38*). Ca(A/A70*f*) composite beads were first exposed to 0.05 wt% PLL (15-30k) for 1 min, followed by exposure to 0.5 wt% PLL (4-15k) for 6 min, and after a saline wash step, by the usual final coat with 0.03 wt% Alg for 4 min. The resulting capsules, after manual cutting and exposure to Na citrate and 2M NaCl, show both the presence of a distinct outer shell formed by reaction of the higher MW PLL with A70*f* near the surface, and core-cross-linking between the lower MW PLL and residual A70*f* remaining in the core (Figure 15, a-c). In contrast, the capsules prepared using only 0.5 wt% PLL (4-15k) did not show a similarly distinct outer shell (Figure 13c). This demonstrates the ability to exert some control over shell and core cross-linking, and may allow independant tuning the MW cut-off and bead strength.

In-Vitro Cell Viability

C_2C_{12} mouse cells were encapsulated in APA, the shell-cross linked (A/A70)P(15-30k, 0.05 wt%)A and the core-crosslinked (A/A70)P(4-15k, 0.5 wt%)A capsules at a rate of 2 million cells per ml capsules. The capsules were then cultured in DMEM (with 10% FBS) *in vitro* for one week. The appearance of cell-containing APA and shell or core-cross linked (A/A70)PA capsules are similar as is shown in Figure 3. The numbers of living cells per microcapsule were monitored versus time of *in vitro* incubation, using the Alamar Blue assay. Figure 16a shows that the average live cell numbers in these shell-crosslinked capsules are initially slightly lower than those in APA microcapsules at day 1 and 4. However, a reasonable number of cells are viable, there is good proliferation and the number of live cells exceed those in APA capsules by day 7, indicating that the A70 in the core of the shell cross-linked (A/A70)PA capsules is not detrimental to cell viability.

Figure 16b shows the cell viability in terms of the average number of live cells per core-cross linked (A/A70)PA and APA capsule after 1, 3, 5 and 7 days. The comparison show that the live cell numbers are higher for APA capsules, though similar relative increases in cell numbers (50-60%) are seen for both types of capsule. Comparison with the good cell viabilities observed in the case of analogous shell-cross linked capsules prepared using only 0.05 wt% PLL (15-30k) (Figure 16a) suggests that the lower initial cell viability in the present core cross-linked capsules is due to the larger amount of lower MW PLL used, perhaps just indirectly through formation of the cross-linked core that interferes with proliferation of the cells.

It was at first surprising that the diffusion of PLL into the capsule core does not have a more negative effect on cell viability. The preferred location of PLL*r* (4-15k) in the shell, compared to the homogeneous distribution of A70*f* (Figure 5) obviously reflects the fact that PLL is applied from the outside, while A70 is found throughout the core. PLL in the bead core should not be very toxic towards the encapsulated cells, as verified by the data in Figure 16b, because most of the PLL diffusing in from the outside should rapidly react with the A70 present throughout the core. Any residual unreacted PLL would likely be complexed by alginate, and thus rendered much less cytotoxic, as reported previously for the complexes formed between polystyrenesulfonate and polycations (*63*).

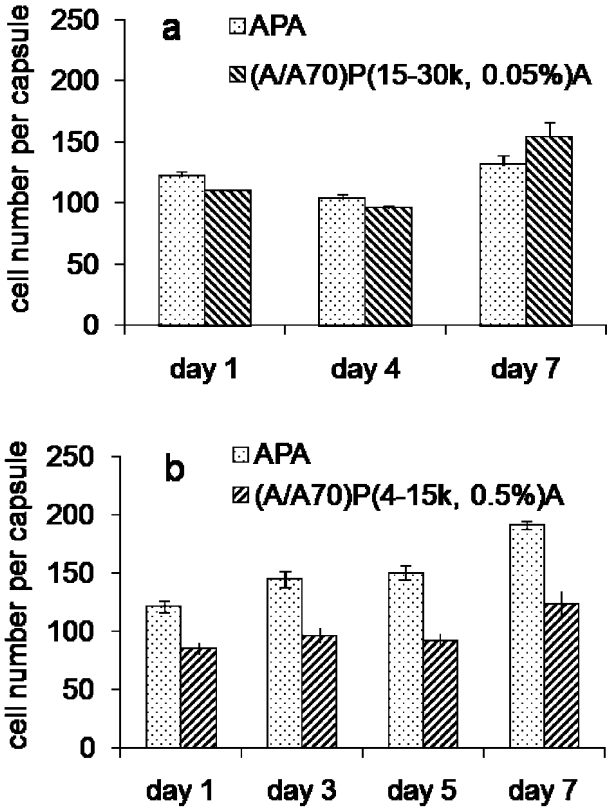

Figure 16. In vitro cell viability of C_2C_{12} cells encapsulated in APA and (A/A70)PA capsules over time. a) APA and shell-cross linked (A/A70)P(15-30k, 0.05 wt %)A capsules and b) APA and core-cross linked (A/A70)P(4-15k, 0.5 wt %)A capsules. Error bars show the standard deviation.

Mechanical Stability of APA and Core-Cross Linked Capsules

The mechanical stability of APA and core cross-linked (A/A70)PA capsule was determined using a high strain rate micro compression tester. It was used to measure the maximum load before rupture, applied through a stepper motor at a constant speed of 10 μm/s to the maximum load while plotting the force registered against vertical displacement. Figure 17 shows a typical force versus displacement curve, for compressing a single APA and core cross-linked (A/A70)PA capsules. During the experiments, the force transducer probe started to move downward at point 1 and touched the capsule at point 2. The compression commenced immediately and the force started to increase until the capsule under went rupture (point 3). Upon compression, the beads deformed to between 2 and 2.5 times their original diameter, and about 20 to 25% of their original height, before cracking. It was noted that the present core-cross linked (A/A70)PA capsules, upon exceeding their maximum compressive loading, do not undergo

In Polymeric Delivery of Therapeutics; Morgan, S., et al.;
ACS Symposium Series; American Chemical Society: Washington, DC, 2010.

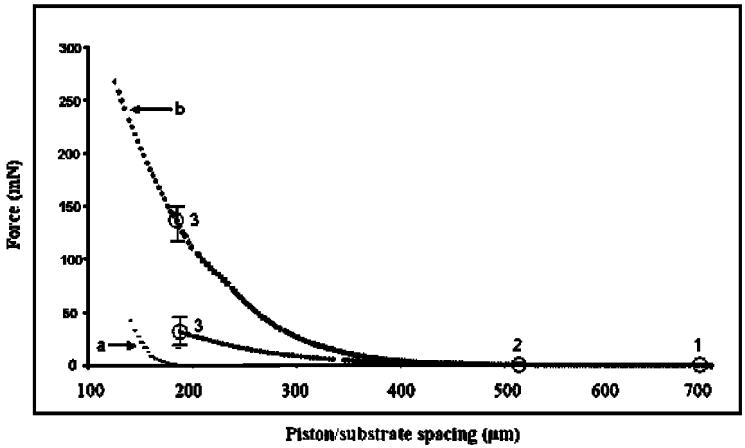

Figure 17. Force versus displacement curve obtained from compression of a) APA, b) core cross-linked (A/A70) PA capsule. The diameter of the microcapsule was about 500 μm.

catastrophic failure, but rather undergo progressive cracking that still provides some matrix isolation for the cells embedded in the fragments. This is in contrast to APA core-shell capsules that fail by a catastrophic bursting mechanism, which exposes all of the bead content to the host.

Typically, core cross-linked capsule exhibited a first crack about 120-150 mNewtons of compressive force (Figure 17). Compression of the same type of capsule after extraction of the calcium in the core with Na citrate shows a slight reduction (data not shown) in load at failure, indicating that most of the bead strength derives from the synthetic polymer network, rather than from the CaAlg matrix. Extraction with citrate is designed to mimic the slow exchange of calcium for sodium known to take place in tissue. The results indicate that the bead strength of these covalently cross-linked capsules should not suffer from such ion exchange. In contrast, typical force at failure for non-cross linked APA capsules described here is between 20 and 40 mNewtons, with the failure mechanism resembling the sudden bursting of a balloon, rather than progressive cracking (Figure 17).

MW Cut-Off of APA and Composite Cross Linked Capsules

It is important that capsules containing cells allow the diffusion of nutrients and metabolites, while preventing the ingress of components of the host immune system. The ideal MW cut-off of the capsule membrane is one that is designed to keep high MW molecules such as antibodies and immunoglobulins out, while allowing exchange of oxygen, nutrients and metabolites including the specific enzymes needed by the patient. The metabolic requirements of various cell types are different and, hence, optimal membrane permeability is expected to depend on the choice of cells, with values of about 100 - 200 kDa commonly considered to be suitable for allografts (*64–67*).

In Polymeric Delivery of Therapeutics; Morgan, S., et al.;
ACS Symposium Series; American Chemical Society: Washington, DC, 2010.

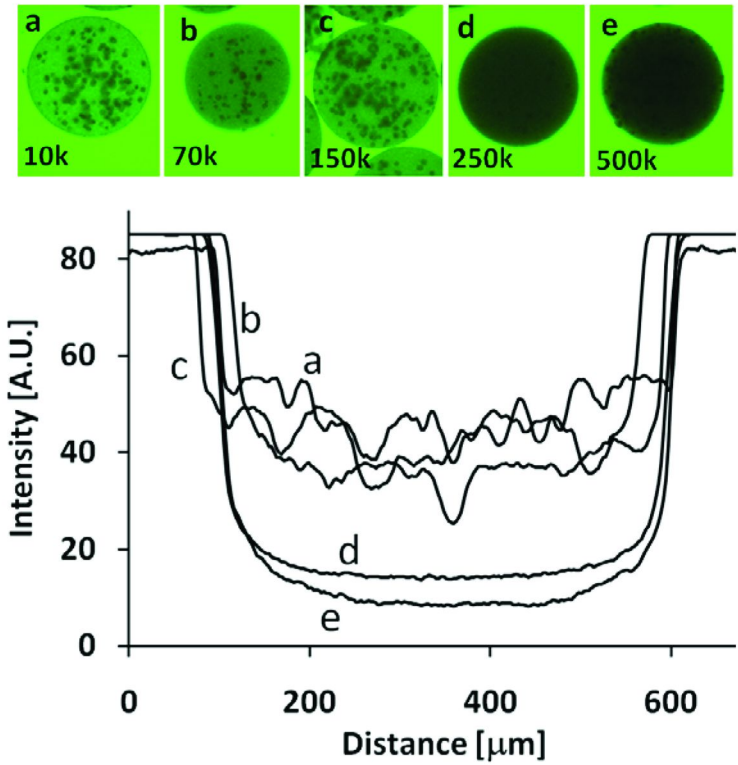

Figure 18. Top: CLSM middle sections of cell containing (A/A70)P(4-15k, 0.5 wt%)A(0.03 wt%) capsules exposed for 24h at room temperature to 0.05 wt% dextran-FITC with nominal MWs of a) 10k, b) 70k, c) 150k, d) 250k, and e) 500k. Bottom: Line profile from images as above.

The MW cut-off of these new shell- and core-cross linked capsules was estimated using a series of commercial dextran-FITC samples with nominal MWs of 10, 70, 150, 250 and 500 kDa (*6*, *68*). Dextran is a polysaccharide composed of glucose units, and fluorescein- labelled dextrans (*69*) have been used to examine the permeability of various membranes, microcapsules and cells. Commercial dextran-FITC samples were analysed by GPC using linear PEG as standard. GPC analysis showed polydispersity indices of about 2 except for the 150 kDa sample, which has a much larger polydispersity index of 4.7. This broad MW distribution led to significant in-diffusion of the low MW fraction. In addition, dextran may behave differently than globular proteins in solution, and as such the use of dextran-FITC provides only a rough indication of the MW cut-off.

The shell-cross linked capsules were exposed to 0.0015 wt% dextran-FITC solutions for 24h and then examined by CLSM. The results showed increasing in-diffusion with decreasing MW, similar to control APA capsules (data not shown). Similarly, core-cross linked capsules containing C_2C_{12} mouse myoblast cells were tested by CLSM following 24h exposure to dextran-FITC (0.05 wt%) having different MWs. Figure 18 shows that dextrans of 500 and 250 kDa are

almost completely excluded, while dextrans having MW's of 10 and 70 kDa can diffuse in freely. The 150 kDa dextran has a much broader MW distribution than the other four dextran studied, including a large low MW fraction, which is considered to be responsible for most of the interior fluorescence observed in Figure 18c. Overall, the results indicates that the shell and core cross linked capsules have MW cut offs around 100-200 kDa, similar to APA capsules (data not shown), and is considered suitable for immuno-isolation in allo-transplants.

The permeability of APA and shell-crosslinked capsules containing cells was also assessed by looking for the uptake of BSA*f* (MW 66 kDa) (data not shown). Both types of capsules were permeable to BSA*f*, indicating a MW cut-off greater than 70 kDa, consistent with the dextran-FITC results.

Conclusion

We have shown that covalently cross-linked shells can be formed around CaAlg beads by the sequential deposition of oppositely charged polyelectrolytes bearing complementary amine and acetoacetate reactive groups. We have also shown that internally and externally cross-linked networks can be formed in CaAlg beads by inclusion of A70 in conventional APA-type capsule cores, and exposure to sufficient amounts of PLL having appropriate MW. The distribution of the polyelectrolytes in the capsules was studied using fluorescently labeled analogs. Capsule resistance to citrate and 2M NaCl/0.1M NaOH was used to demonstrate the cross-linked nature of the cores and shells. These capsules also have greater resistance to chemical and mechanical stress tests, compared to control APA capsules. The MW cut-off of cross-linked capsules was shown to be similar to that of the control APA capsules, and is suitable for cell encapsulation. The *in vitro* and *in vivo* viability of encapsulated C_2C_{12} cells within shell and/or core cross-linked capsules was similar to that of conventional APA capsules.

In summary, these results describe promising new approaches to cell encapsulation that offer enhanced capsule resistance to chemical and mechanical stresses, while preserving the desired biocompatibility, and may ultimately be useful for clinical immunosuppressive therapies.

Acknowledgments

The authors of this chapter would like to thank the Canadian Institutes for Health Research (CIHR) and the Natural Sciences and Engineering Research Council (NSERC) of Canada for supporting this work.

References

1. Chang, T. M. S. *Science* **1964**, *146*, 524–525.
2. Bañó, M. C.; Cohen, S.; Visscher, K. B.; Allcock, H. R.; Langer, R. *Nat. Biotechnol.* **1991**, *9*, 468–471.
3. Uludag, H.; Sefton, M. V. *Biotechnol. Bioeng.* **1992**, *39*, 672–678.

4. Thu, B.; Bruheim, P.; Espevik, T.; Smidsrød, O.; Soon-Shiong, P.; Skjåk-Bræk, G. *Biomaterials* **1996**, *17*, 1031–1040.
5. Lim, F.; Sun, A. M. *Science* **1980**, *210*, 908–910.
6. Vandenbossche, G. M. R.; Van Oostveldt, P. V.; Demeester, J.; Remon, J.-P. *Biotechnol. Bioeng.* **1993**, *42*, 381–386.
7. Schneider, S.; Feilen, P. J.; Brunnenmeier, F. *Diabetes* **2005**, *54*, 687–693.
8. Peirone, M. A.; Delaney, K.; Kwiecin, J.; Fletch, A.; Chang, P. L. *Hum. Gene Ther.* **1998**, *9*, 195–206.
9. Van Raamsdonk, J. M.; Cornelius, R. M.; Brash, J. L.; Chang, P. L. *J. Biomater. Sci., Polym. Ed.* **2002**, *13*, 863–884.
10. Rokstad, A. M.; Holton, S.; Strand, B.; Steinkjer, B.; Ryan, L.; Kulseng, B.; Skjak-Braek, G.; Espevik, T. *Cell Transplant.* **2002**, *11*, 313–324.
11. Zimmermann, H.; Zimmermann, D.; Reuss, R. *J. Mater. Sci., Mater. Med.* **2005**, *16*, 491–501.
12. Lanza, R. P.; Kuhtreiber, W. M.; Ecker, D.; Staruk, J. K.; Chick, W. L. *Transplantation* **1995**, *59* (10), 1377–1384.
13. Soon-Shiong, P.; Heintz, R. A.; Skjåk-Bræk, G. Microencapsulation of cells. U.S. Patent 5,762,959, 1998.
14. Zekorn, T.; Siebers, U.; Horcher, A.; Schnettler, R.; Klock, G.; Bretzel, R. G.; Zimmerman, U.; Federlin, K. *Transplant. Proc.* **1992**, *24*, 937–939.
15. Lanza, R. P.; Kuhtreiber, W. M.; Ecker, D.; Staruk, J. K.; Chick, W. L. *Transplantation* **1995**, *59* (10), 1377–1384.
16. Mørch, Y. A.; Donati, I.; Strand, B. L.; Skjåk-Bræk, G. *Biomacromolecules* **2006**, *7*, 1471–1480.
17. Darrabie, M. D.; Kendall, W. F., Jr.; Opara, E. C. *Biomaterials* **2005**, *26*, 6846–6852.
18. Chandy, T.; Mooradian, D. L.; Rao, G. H. R. *J. Appl. Polym. Sci.* **1998**, *70*, 2143–2153.
19. Bünger, C. M.; Gerlach, C.; Freier, T.; Schmitz, K. P.; Pilz, M.; Werner, C.; Jonas, L.; Schareck, W.; Hopt, U. T.; De Vos, P. *J. Biomed. Mater. Res.* **2003**, *67A*, 1219–1227.
20. Haque, T.; Chen, H.; Ouyang, W.; Martini, C.; Lawuyi, B.; Urbanska, A. M.; Prakash, S. *Mol. Pharmaceutics* **2005**, *2*, 29–36.
21. Gaserod, O.; Smidsrod, O.; Skjak-Braek, G. *Biomaterials* **1998**, *19*, 1815–1825.
22. Leung, A.; Lawrie, G.; Nielson, L. K.; Trau, M. *J. Microencapsulation* **2008**, *25*, 387–398.
23. Wang, Y. *J. Mater. Sci. Eng C.* **2000**, *13*, 59–63.
24. Schneider, S.; Feilen, P. J.; Slotty, V.; Kampfner, D.; Preuss, S.; Berger, S.; Beyer, J.; Pommersheim, R. *Biomaterials* **2001**, *22*, 1961–1970.
25. Vallbacka, J. J.; Sefton, M. V. *Tissue Eng.* **2007**, *13* (9), 2259–2269.
26. Mokry, J.; Karbanova, J.; Lukas, J.; Paleckova, V.; Dvorankova, B. *Biotechnol. Prog.* **2000**, *16*, 897–904.
27. Smeds, K. A.; Grinstaff, M. W. *J. Biomed. Mater. Res.* **2001**, *54*, 115–121.
28. Hubbell, J. A.; Pathak, C. P.; Sawhney, A. S.; Desai, N. P.; Hossainy, S. F. A.Gels for encapsulation of biological materials. U.S. Patent 5,529,914, 1996.

29. Soon-Shiong, P.; Desai, N. P.; Sandford, P. A.; Heintz, R. A.; Sojomihardjo, S.Crosslinkable polysaccharides, polycations and lipids useful for encapsulation and drug release. U.S. Patent 5,837,747, 1998.
30. Rokstad, A. M.; Donati, I.; Borgogna, M.; Oberholzer, J.; Strand, B. L.; Espevik, T.; Skjåk-Braek, G. *Biomaterials* **2006**, *27*, 4726–4737.
31. Wang, M.; Childs, R. F.; Chang, P. L. *J. Biomater. Sci., Polym. Ed.* **2005**, *16*, 91–113.
32. Araki, T.; Hitchcock, A. P.; Shen, F.; Chang, P. L.; Wang, M.; Childs, R. F. *J. Biomater. Sci., Polym. Ed.* **2005**, *16*, 611–627.
33. Chandy, T.; Mooradian, D. L.; Rao, G. H. R. *Artif. Organs* **1999**, *23*, 894–903.
34. Dusseault, J.; Leblond, F. A.; Robitaille, R.; Joudan, G.; Tessier, J.; Menard, M.; Henly, N.; Halle, J.-P. *Biomaterials* **2005**, *26*, 1515–1522.
35. Leblond, F. A.; Halle, J.-P. U.S. Patent Appl. Publ., 2005, 22pp, US 2005147594 A1 20050707, CAN 143: 103356 AN 2005: 591961.
36. Dusseault, J.; Langlois, G.; Meunier, M. –C.; Menard, M.; Perreault, C.; Halle, J.-P. *Biomaterials* **2008**, *29*, 917–924.
37. Crooks, C. C.; Douglas, J. A.; Broughton, R. L.; Sefton, M.V. *J. Biomed. Mater. Res.* **1990**, *24*, 1241–1262.
38. Prokop, A.; Hunkeler, D.; Powers, A. C.; Whitesell, R.; Wang, T. G. *Adv. Polym. Sci.* **1998**, *136*, 53–73.
39. Sakai, S.; Hashimoto, I.; Kawakami, K. *Biochem. Eng. J.* **2006**, *30*, 76–81.
40. Prakash, S.; Martoni, C. *Appl. Biochem. Biotechnol.* **2006**, *128*, 1–21.
41. Hertzberg, S.; Moen, E.; Vogelsang, C.; Østgaard, K. *Appl. Microbiol. Biotechnol.* **1995**, *43*, 10–17.
42. Prokop, A.; Hunkeler, D.; Dimari, S.; Haralson, M. A.; Wang, T. G. *Adv. Polym. Sci.* **1998**, *136*, 1–51.
43. Wang, T.; Lacik, T.; Brissova, M.; Anilkumar, A. V.; Prokop, A.; Hunkeler, D.; Green, R.; Shahrokhi, K.; Powers, A. C. *Nat. Biotechnol.* **1997**, *15*, 358–362.
44. Donati, I.; Haug, I. J.; Scarpa, T.; Borgogna, M.; Draget, K.I.; Skjåk-Bræk, G.; Paoletti, S. *Biomacromolecules* **2007**, *8*, 957–962.
45. Mazumder, M. A. J.; Shen, F.; Burke, N. A. D.; Potter, M. A; Stöver, H. D. H. *Biomacromolecules* **2008**, *9*, 2292–2300.
46. Shen, F.; Mazumder, M. A. J.; Burke, N. A. D.; Stöver, H. D. H.; Potter, M. A. *J. Biomed. Mater. Res., Part B* **2009**, *90B*, 350–361.
47. Mazumder, M. A. J.; Burke, N. A. D.; Shen, F.; Potter, M. A.; Stover, H. D. H. To be submitted.
48. Mazumder, M. A. J.; Burke, N. A. D.; Shen, F.; Potter, M. A.; Stover, H. D. H. *Biomacromolecules* **2009**, *10*, 1365–1373.
49. Holme, H. K.; Davidsen, L.; Kristiansen, A.; Smidsrød, O. *Carbohydr. Polym.* **2008**, *73*, 656–664.
50. Ross, C. J. D.; Bastedo, L.; Maier, S. A.; Sands, M. S.; Chang, P.L. *Hum. Gene Ther.* **2002**, *11*, 2117–2127.
51. Li, A. A.; Shen, F.; Zhang, T.; Cirone, P.; Potter, M.; Chang, P. L. *J. Biomed. Mater. Res., Part B* **2006**, *77*, 296–306.

52. Burke, N. A. D.; Mazumder, M. A. J.; Hanna, M.; Stöver, H. D. H. *J. Polym. Sci., Part A: Polym. Chem.* **2007**, *45*, 4129–4143.
53. Bysell, H.; Malmsten, M. *Langmuir* **2006**, *22*, 5476–5484.
54. Shen, F.; Li, A. A.; Gong, Y-K.; Somers, S.; Potter, M. A.; Winnik, F. M.; Chang, P. L. *Hum. Gene Ther.* **2005**, *16*, 971–984.
55. Strand, B. L.; Morch, Y. A.; Espevik, T.; Skjak-Braek, G. *Biotechnol. Bioeng.* **2003**, *82* (4), 386–394.
56. Ross, C. J. D.; Bastedo, L.; Maier, S. A.; Sands, M. S.; Chang, P. L. *Hum. Gene Ther.* **2002**, *11*, 2117–2127.
57. Thu, B.; Gåserød, O.; Paus, D.; Mikkelson, A.; Skjåk-Bræk, G.; Toffanin, R.; Vittur, F.; Rizzo, R. *Biopolymers* **2000**, *53*, 60–71.
58. Velings, N. M.; Mestdagh, M. M. *Polym. Gels Networks* **1995**, *3*, 311–330.
59. Goosen, M. F. A.; O'Shea, M.; Gharapetian, H. M.; Chou, S.; Sun, A. M. *Biotechnnol. Bioeng.* **1985**, *27*, 146–150.
60. King, G. A.; Daugulis, A. J.; Faulkner, P.; Goosen, M. F. A. *Biotechnol. Prog.* **1987**, *3*, 231–240.
61. Gåserød, O.; Smidsrød, G.; Skjåk-Bræk, G. *Biomaterials* **1998**, *19*, 1815–1825.
62. 70 mM Na citrate was found to be sufficient to extract calcium from CaAlg beads.
63. Vogel, M. K.; Cross, R. A.; Bixler, H. J.; Guzman, R. J. *J. Macromol. Sci. Chem. A* **1970**, *4*, 675–692.
64. Morris, P. J. *Trends Biotechnol.* **1996**, *14*, 163–167.
65. Grigorescu, G.; Rehor, A.; Hunkeler, D. *J. Microencapsulation* **2002**, *19*, 245–259.
66. Qi, W.; Ma, J.; Liu, Y.; Liu, X.; Xiong, Y.; Xie, Y.; Ma, X. *J. Membr. Sci.* **2006**, *269*, 126–132.
67. Xing, Z. C.; Huh, M. W.; Kang, I. K. *Key Eng. Mater.* **2007**, *342−343*, 417–420.
68. Vandenbossche, G. M. R.; Oostveldt, P. V.; Remon, J. P. *J. Pharm. Pharmacol.* **1991**, *43*, 275–27.
69. De Belder, A. N.; Granath, K. *Carbohydr. Res.* **1973**, *30*, 375–378.